FATIGUE CRACK PATHS AND RESIDUAL STRESSES IN COLD FORMED RECTANGULAR STRUCTURAL TUBES

Sami Heinilä[1], Timo Björk[1], Gary Marquis[1], Mika Bäckström[2], and Reijo Ilvonen[3]
[1]Lappeenranta University of Technology, P.O. Box 20, FIN-53851, Lappeenranta, Finland
[2]VTT Industrial Systems, [2]P.O. Box 1700, FIN-02044 VTT, Finland
[3]Rautaruukki Metform, Harvialantie 420, FIN-13300 Hämeenlinna, Finland
Author for correspondence: sami.heinila@lut.fi

Abstract

Global bending loads in rectangular hollow section (RHS) structural beams create transverse bending stresses along the inside corners of the tubes. In some design applications the fatigue strength of the inside corner becomes critical. Fabricators often desire smaller corner radii both for ascetic reasons and to reduce the machining preparation required for some welded joint configurations. However, smaller corner radii can cause higher residual stresses in the corners and increased fatigue susceptibility due to the larger stress concentration factor. High degrees of cold forming also increase the risk of microcracking. To better understand this behaviour and to help develop guidelines both for RHS manufacturers and end-users, both numerical modelling and fatigue experiments have been performed. Experiments included both full-scale RHS beam testing and testing of RHS sections. The residual stress pattern produced by cold forming has been modelled using elastic-plastic finite element analysis. Predicted residual stresses are consistent with measured values. Fatigue experiments and fracture mechanics analyses have shown that both the fatigue crack growth path and the fatigue life are greatly influenced by the through thickness residual stresses.

Introduction

A high-strength cold-formed rectangular hollow section structural beam (CFRHS) subjected to cyclic bending loading was found to fail due to fatigue. Applied load and restraint in this case can be modelled as shown in Fig. 1. Initially small discrete flaws along the inner surface of the tube corners grew both in the longitudinal and transverse directions forming one long fatigue crack. Longitudinally, the crack was near the centre support where bending moment was greatest. The crack initiated on the inner surface in the centre of the corner as seen in Fig. 2. As the crack grew in the transverse direction, it gradually turned towards the neutral plane. Eventually the crack path returned to the original direction towards the outer surface forming an S-shaped crack path as seen in the figure. The crack was visible only after it had grown through the wall of the tube. The CFRHS beam material in this case was a fine-grained high-strength structural steel S 650 MC with nominal yield strength of 650 N/mm^2.

Laboratory experiments

Small scale specimens

Bäckström *et al*. [1] have reported fatigue results for constant amplitude tensile loading fatigue of mild steel CFRHS beam sections. The reported yield stress for the material was 355 N/mm^2. All specimens were cut from tubes manufactured according to appropriate EN

CFRHS standards and were purchased randomly from a wholesaler. Constant amplitude tensile loading was applied with stress ratio R = 0.1. A total of 28 pieces were tested. Bäckström *et al*. reported nearly straight crack paths. In this case, however, the external loading constraint produced nearly pure bending in the corner where the crack initiated.

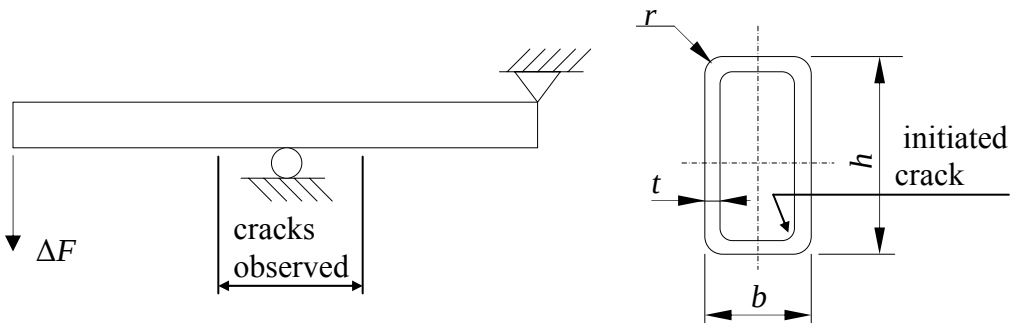

FIGURE 1. Loading, supports and section profile.

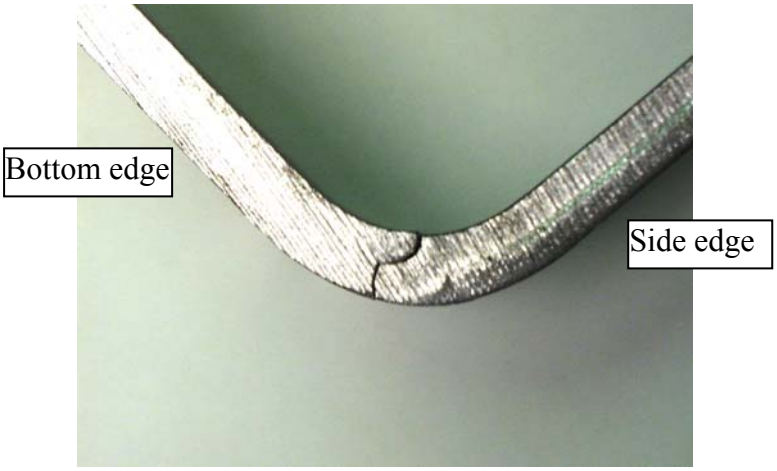

FIGURE 2. Fatigue crack grown through the wall.

Large-scale beam testing

To obtain results more closely resembling the in-service load case, laboratory testing using two CFRHS full-scale beams was performed. The beams were loaded simultaneously with R = 0.5 constant amplitude as shown in Fig. 3. Tests continued until cracks propagating through the tube wall were clearly observed. Different local stress amplitudes were applied. In two beams the residual stresses were removed by heat treatment. A total of eight (8) specimens provided by the manufacturer were tested.

Precise dimensions of the rectangular profile and the initial residual stresses were measured prior to the laboratory tests. Initial residual stresses were measured from inner and outer surfaces of the tubes using the X-ray diffraction method. The measurements showed yield strength magnitude tensile residual stresses on the inner surface. The outer surface had significantly lower compressive residual stresses. The residual stress state was assumed to form due to very high degree of plastic deformation of the corners during the cold-forming process. The magnitude of the residual stresses is also dependent on the yield strength of the material.

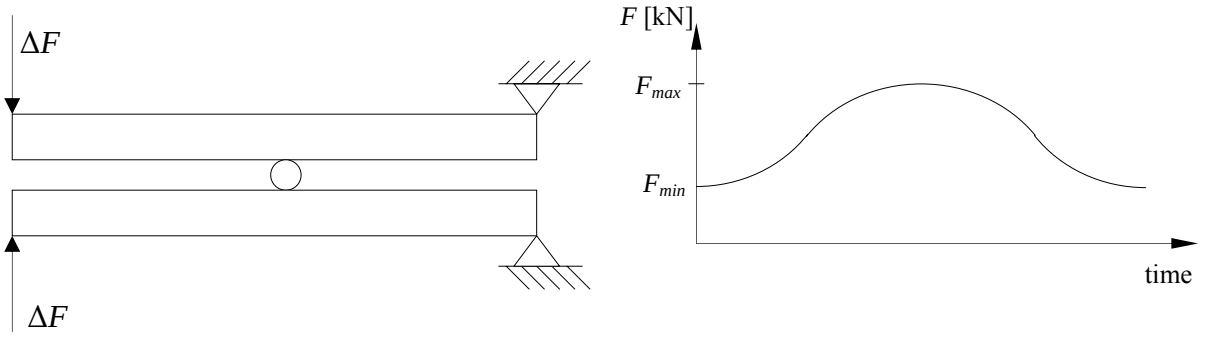

FIGURE 3. Testing configuration and applied loading.

Close inspections of random samples taken from the CFRHS corners prior to laboratory testing showed clear initial flaw-like cavities on the inner surface of the corner as can be seen in Fig 4. In the tests reported by Bäckström *et al*. [1], some of the specimens had initial surface notches on the inside corner caused by considerable corrosion (identified as series B) while others had a relatively smooth surface (identified as series A).

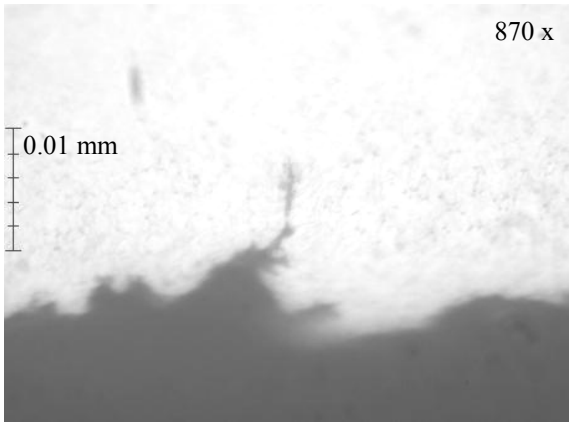

FIGURE 4. Initial flaw in the centre of inner surface of corner.

Finite element analysis

Cold forming simulation

Because the initial residual stress field through the wall thickness could not be accurately measured, elastic-plastic FE analysis was chosen as a means of estimating the residual stress field accumulated during the cold-forming process. In reality the cold-forming operation is a continuous longitudinal process. In this analysis a 2D plane strain assumption was made. This, in practice, simulates the entire length of the CFRHS beam being simultaneously formed. The important longitudinal strains were neglected and would need to be included in a more precise analysis. However, the shape of the tangential residual stress distribution through wall thickness in the region of the corners was obtained. Predicted surface residual stresses were in good agreement with the X-ray diffraction measurements.

The material model used in the cold forming simulation was based on data provided by the CFRHS beam manufacturer. Isotropic hardening was assumed for the cold forming process and five-segment multi-linear stress-strain curve was assumed.

The effect of the residual stress field on the curved crack path and the redistribution of residual stresses with crack growth were of interest. 2D plane strain FE-based fracture mechanics based crack path analysis was performed. The previously simulated residual stress pattern for the formed profile was assumed as the initial condition. Because of the complex residual stress fields, crack simulation programs could not be used and mesh regeneration with crack advance was not employed. Stress intensity factor results were obtained from ordinary elements that could not account for stress singularities. This reduced the precision of the FE-analyses, but results were valuable for investigating trends in the data and for making general comparisons to the experimental data.

Crack path evaluation

Mode I and Mode II stress intensity factors along two different crack paths were analysed. In both cases the crack path was predetermined based on experimental observations and a suitable FE mesh was generated prior to the cold forming simulation. Separate FE models were therefore needed for both the straight and S-shape crack paths. Thus, a single FE mesh model could be used for both the cold-forming simulation and the crack growth analysis. Several attempts were required to obtain a single mesh that was suitable for both the cold forming and crack propagation processes. One simulated crack path was similar to the path shown in Fig. 1 and the other one was a straight line across the corner (Fig. 5).

The FE models were constructed using quadratic 2D elements. No special quarter distance crack tip elements were used since the crack had to advance and no remeshing capability was available. Crack growth was simulated by disconnecting nodes from the path as the crack advanced. After each node disconnection process, the current displacement field and residual stress field was calculated.

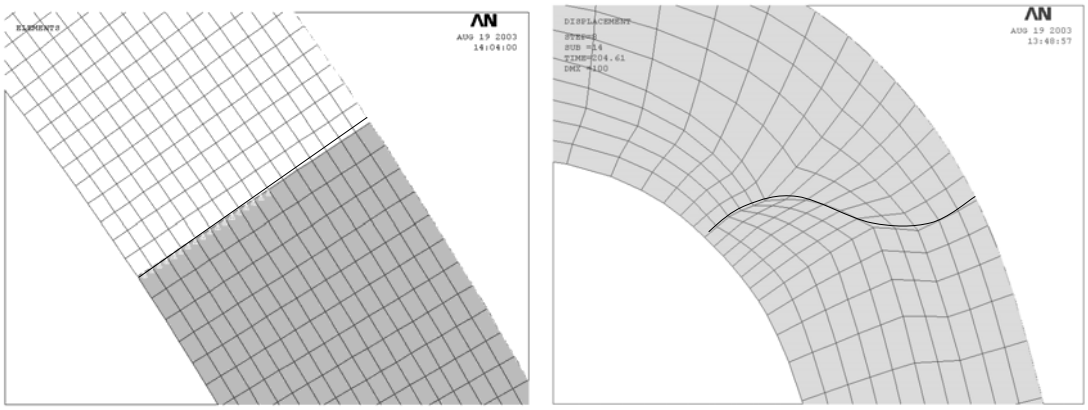

FIGURE 5. Two different crack paths modelled a) straight crack and b) S-shaped crack.

Results

Cold-forming simulation

The cold-formed shape of the RHS beam was not quite met due to lack of the third dimension in the analysis. Since the longitudinal strains in real structure would enforce the elastic spring back the final shape of the simulated body was slightly over deformed.

Crack paths

The crack paths were analysed step by step. The idea was to see how the residual stress field would affect the advancing crack direction. The external loading was supposed to have created these two different crack paths step by step and be zero at the moment of observation. The curving crack was observed in the laboratory tests although the test was stopped before the crack had grown through (Fig. 6).

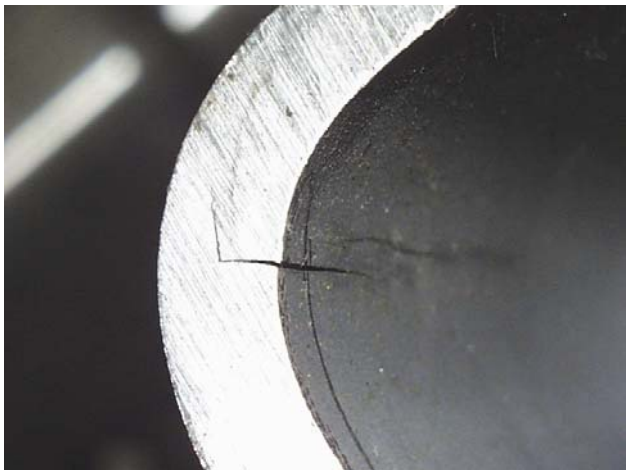

FIGURE 6. Crack path obtained from the laboratory test.

Residual stress distribution

The residual stress distribution (Fig. 7) was consistent with the measured data. However, due to the fact that the stress state is not plane strain even in the middle of the beam during the forming process but triaxial instead, the numerical values differ significantly from the measured values.

In curved crack case the residual stress field redistributes in a way that there is always a tensile stress peak in front of the crack tip transverse to the direction of the crack propagation direction.

In straight crack case the tensile stress dies away gradually before the crack tip advances into the compressive stress field.

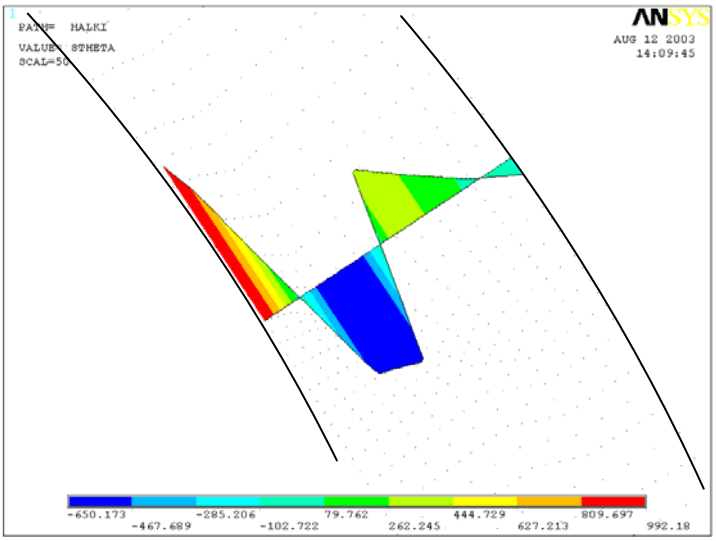

FIGURE 7. Predicted through-thickness residual stress distribution after cold forming.

Stress intensity factors of the different crack paths

The two different crack paths were analysed for finding out whether they are even possible and what happens to the residual stress field as the crack propagates. The most important result describing the behaviour of the crack, however, is the progression of the stress intensity factors (SIF) K_I and K_{II} (Fig. 8).

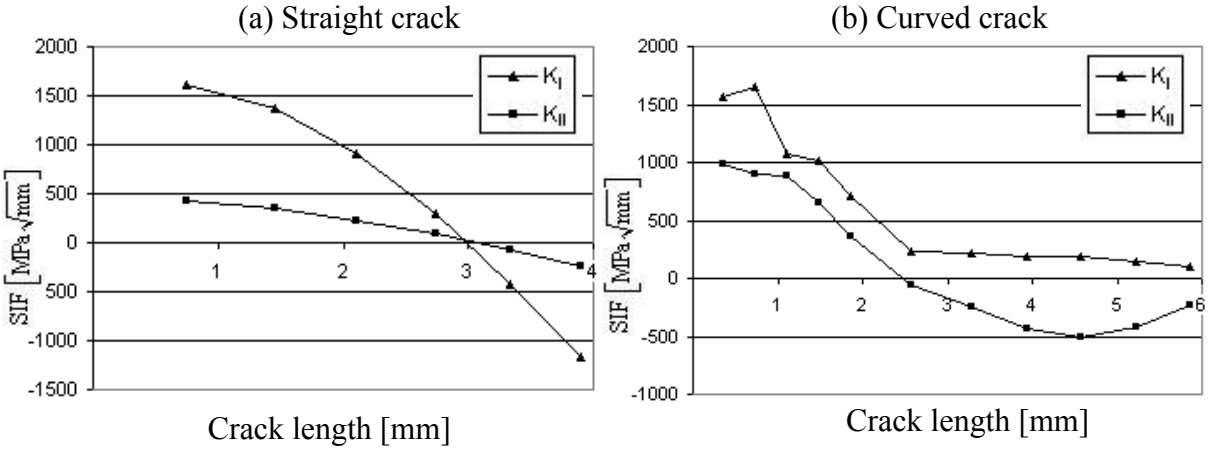

FIGURE 8. Stress intensity factors for straight (a) and curved crack (b) in case of no loading.

The SIF values in Fig. 8 are obtained when the crack length is adjusted manually and the current residual stress field is let to redistribute. In other words it is assumed that the crack had grown up to the current step due to the external loading, the external loading is set to zero, and the residual stresses and the stress intensity factors are calculated at the new crack tip position. Since the external loading was tensile in straight crack case both the K_I and K_{II} values, obtained when the external loading was zero, are minimum SIF values. In curved crack case the external loading was compressive and thus the K_I values are maximum values. The external shear loading is actually to same direction as mode II residual stresses at short cracks. Thus K_{II} values are the minimum values in curved crack case.

In case where the external loading causes bending in the corner of a CFRHS, the crack path would be dominated by the external mode I loading, forcing the crack to grow straight (Fig. 8 a). Since $K_{I\,\min}$ is positive in the early stages of crack growth even moderate external forces can raise the ΔK values above the threshold value. As $K_{I\,\min}$ approaches zero the $K_{I\,\max}$ would have to be greater for getting the crack to open and propagate. At this stage, however, the crack is already long compared to the initial length and thus the $K_{I\,\max}$ is higher even though the external force has not changed.

At longer crack lengths $K_{I\,\min}$ diminishes and eventually becomes zero. In the Fig. 8 a, the $K_{I\,\min}$ can be seen going below zero which does not have a physical meaning. It simply states that the crack would be closed when no external force is acting (i.e. $K_{I\,\min} = 0$). It is worth noting that the $K_{II\,\min}$ is approximately 1/3 of the $K_{I\,\min}$ value in each stage of the crack growth.

In the other crack path case where the external loading causes more shearing in the corner of a CFRHS the crack path would be affected by the residual stress field inside the CFRHS (Fig. 8 b). In the large-scale beam test configuration the centre support creates a high local stress concentration consisting of both global bending and local shear stresses. The shear loading enables the crack to grow in mode II. It must be noted that the external loading is compressive thus making the crack growth impossible in mode I without the residual stresses.

If the external mode I loading is not sufficient for opening the crack tip, as is the case with compressive loading, the residual stresses would have to be high enough to enable the crack growth in mode I. Otherwise, the crack would have to find another growth mode, which in this case would be mode II. After all, if the crack grew straight, the crack would have to grow through the compressive residual stress field, and as the external force is also compressive, the growth in mode I is not possible. Therefore the growth is governed by mode II instead.

Both the external loading and the residual stress drive the crack growth in the same direction. In this case the superposition of the external loading and the residual stress mode II stress intensity factor $K_{II\,\max}$ is higher than K_{II} purely from the residual stress (Fig. 8 b). Mode I superposition does not change $K_{I\,\max}$ as in the Fig. 8 b, since the external mode I loading is compressive. The actual ratio between K_{II} and K_I is therefore higher than in the Fig. 8 b. Either of the SIF values is not constant and eventually $K_{II\,\min}$ becomes zero and negative. This indicates the crack changing its direction near half wall thickness. At this point mode I crack growth is possible again to initial direction due to the residual stress redistribution and the crack would turn to obtain mode I growth again.

Summary

The corners of the CFRHS beams may be critical to fatigue cracking in several applications. In the future when the weld quality is high enough this should be taken into account for welded structures as well. Even the compressive external loading is not sufficient to prevent fatigue cracking due to high tensile residual stresses in the inside corner of the CFRHS. The compressive loading combined with the residual stresses causes the crack to change its growth mode rather than prevent the propagation.

The fatigue cracking is particularly displeasing in situations when the observation can only be done from the outer surfaces of the CFRHS beams. In these cases the crack has grown quite a time before it could have been observed and the structure has already reached the end of its fatigue life.

References

1. Bäckström, M., Savolainen, M., Ilvonen R. and Laitinen R. In Proceedings of FATIGUE2002, Stockholm, 2002, 277 – 302